# Magnetic-field and composition tuned antiferromagnetic instability in the quantum spin-liquid candidate $NaYbO_2$

Jie Guo,[1,2] Xinguo Zhao,[1,2,*] Seiko Ohira-Kawamura,[3] Langsheng Ling,[4] Junfeng Wang,[5] Lunhua He,[6,7,8] Kenji Nakajima,[3] Bing Li,[1,2,†] and Zhidong Zhang[1,2]

[1]*Shenyang National Laboratory for Materials Science, Institute of Metal Research, Chinese Academy of Sciences, Shenyang 110016, China*
[2]*School of Materials Science and Engineering, University of Science and Technology of China, Shenyang 110016, China*
[3]*J-PARC Center, Japan Atomic Energy Agency, Tokai, Ibaraki 319-1112, Japan*
[4]*High Magnetic Field Laboratory of the Chinese Academy of Science, Anhui Province Key Laboratory of Condensed Matter Physics at Extreme Conditions, Hefei 230031, China*
[5]*Wuhan National High Magnetic Field Center, Huazhong University of Science and Technology, Wuhan 430074, China*
[6]*Beijing National Laboratory for Condensed Matter Physics, Institute of Physics, Chinese Academy of Sciences, Beijing 100190, China*
[7]*Spallation Neutron Source Science Center, Dongguan 523803, China*
[8]*Songshan Lake Materials Laboratory, Dongguan 523808, China*

(Received 23 March 2020; revised manuscript received 30 April 2020; accepted 27 May 2020; published 11 June 2020)

$NaYbO_2$ has been reported as a possible host for the quantum spin-liquid state. Here, the composition-dependent polycrystalline $Na_{1-x}YbO_2$ ($x = 0$, 0.03, and 0.07) has been investigated by combining high-field magnetizations and inelastic neutron scattering techniques. For the $x = 0$ sample, no signature of a magnetic order is observed down to 0.3 K. Inelastic neutron scattering measurement suggests a continuous low-energy excitation spectrum centered at momentum transfer ($Q$) $\sim 1.25$ Å$^{-1}$ and extending up to energy transfer ($E$) $\sim$ 2.0 meV. In contrast, $x = 0.03$ and 0.07 samples exhibit magnetic transitions at 1.1 and 2.3 K, respectively. High-field magnetization measurements indicate similar behaviors for $x = 0$ and 0.03 samples including plateaulike features at the 1/3 saturated magnetization, which implies that the spin disorder in the $x = 0$ sample might be suppressed preceding the emergence of the up-up-down phase. This composition- and field-dependent study allows us to construct complete phase diagrams indicating that $NaYbO_2$ is a promising candidate for the quantum spin-liquid state in close proximity to the antiferromagnetic instability tuned by the application of magnetic fields as well as controlling the concentration of $Na^+$ ion vacancies.

DOI: 10.1103/PhysRevMaterials.4.064410

## I. INTRODUCTION

Frustrated spin systems are believed to be an ideal playground for the realization of quantum spin liquid (QSL) [1,2]. In a strongly frustrated magnetic system, the competing magnetic interactions that cannot be simultaneously satisfied promote quantum fluctuations and essentially prevent long-range order in the system. While several theoretical models have been proposed [3–6], such as the $Z_2$ and Kitaev models, the realization of QSL in real materials is quite challenging. A number of spin-1/2 triangular-lattice antiferromagnetic (AFM) organic Mott insulators [7,8], such as $\kappa$-(BEDT-TTF)$_2$Cu$_2$(CN)$_3$ and EtMe$_3$Sb[Pd(dmit)$_2$]$_2$, have been widely surveyed for the QSL state. At the same time, their inorganic counterparts have also been investigated extensively. In triangular-lattice AFM $YbMgGaO_4$ [9], effective spins ($J_{\rm eff} = 1/2$) on $Yb^{3+}$ ions do not exhibit trivial long-range order [10,11]. In the kagome lattice $ZnCu_3(OH)_6Cl_2$ [12], long-range order has not been detected down to 20 mK [13], and an inelastic neutron scattering (INS) study has revealed fractionalized excitations [14]. A spin excitation continuum has been probed in the pyrochlore-lattice $Ce_2Zr_2O_7$, indicating the existence of a three-dimensional QSL state [15].

The inorganic compounds $NaYbCh_2$ (Ch = O, S, and Se) have been prepared and studied for magnetic properties and specific heat for several decades [16,17]. Very recently, further measurements down to much lower temperatures have suggested that $NaYbCh_2$ (Ch = O, S, and Se) are a typical $J_{\rm eff} = 1/2$ triangular-lattice AFM system serving as a promising host for QSL [18]. In contrast to $YbMgGaO_4$ with Mg/Ga occupational disorder [19], an absence of inherent structural distortions in this system is manifested in the clear and narrow Yb electron spin resonance (ESR) lines and $^{23}$Na nuclear magnetic resonance (NMR) lines in $NaYbS_2$ [20]. In addition, the crystal-electric-field excitation spectra obtained with INS indicate three shape peaks as expected for $Yb^{3+}$ with the $^2F_{7/2}$ multiplet [20,21], in contrast with $YbMgGaO_4$ where the excitations are broadened and even show one more peak [19]. Very different $g$ factors along and perpendicular to the $c$ axis determined in ESR measurements on single crystals are indicative of a strongly anisotropic quasi-two-dimensional magnetism [20,22,23]. As a critical issue, the fluctuating nature of spins has been confirmed by several

*xgzhao@imr.ac.cn
†bingli@imr.ac.cn

 

muon spin resonance measurements [20,21,24]. Moreover, a continuum excitation spectrum has also been observed in an INS study on powder samples [21,25]. Under high magnetic fields, this system exhibits a series of transitions and there exists a plateaulike feature at the 1/3 saturated magnetization [21–23,25]. *In situ* neutron diffraction experiments support the existence of the up-up-down phase at about 6 T [25,26], in accordance with the specific heat and NMR measurements [22].

Given that the structural intactness may play a critical role in the magnetic behaviors as seen in $YbMgGaO_4$ [11], in this work we present an investigation of polycrystalline $Na_{1-x}YbO_2$ ($x = 0, 0.03$, and 0.07) combining high-field magnetization up to 35 T and INS measurements down to 0.3 K. Spins of the stoichiometric sample are still fluctuating, while the nonstoichiometric ones show well-defined magnetic transitions, but the $x = 0$ and 0.03 samples exhibit similar field-induced cascades. The INS study on $NaYbO_2$ suggests broad low-energy spin excitations. Our research indicates that $NaYbO_2$ has a highly tunable magnetic disordered state close to the AFM instability.

## II. EXPERIMENTAL DETAILS

Polycrystalline samples of $Na_{1-x}YbO_2$ ($x = 0$, 0.03, and 0.07) were synthesized using a solid-state reaction method. $Na_2O$ and $Yb_2O_3$ were carefully grinded into a fine powder and mixed in ratios of 4:1, 3.9:1, and 3.8:1, respectively. Note that appropriate ratios for preparation are highly dependent on the volume of the free space in the crucibles. The mixtures were pressed into solid pellets, sintered at 700 °C for 8 h in magnesia crucibles, and furnace-cooled down to room temperature. The accurate chemical compositions of the final products were examined by means of atomic absorption spectroscopy, which are $NaYbO_2$, $Na_{0.97}YbO_2$, and $Na_{0.93}YbO_2$, respectively. In-house x-ray diffraction was performed to confirm the purity of the samples using a Rigaku D/Max-2000 diffractometer with Cu $K\alpha$ radiation. Neutron powder diffraction measurement was conducted at the General Purpose Powder Diffractor (GPPD) [27] of China Spallation Neutron Source (CSNS) in Dongguan, China, and the collected diffraction patterns were refined using GSAS [28]. The stationary magnetization measurements were carried out using Quantum Design magnetic properties measurement systems (MPMS) in the temperature range from 0.5 to 2 K with a helium-3 cooling system at the High Magnetic Field Laboratory of Chinese Academy of Science and in the temperature range from 1.85 to 380 K with a helium-4 cooling system, respectively. The pulsed-field magnetization measurements were conducted at the magnetization station of the Wuhan National High Magnetic Field Center at up to 35 T. Time-of-flight INS measurements with an incident neutron energy ($E_i$) of 3.135 meV were performed at the cold-neutron disk-chopper spectrometer BL14 AMATERAS of J-PARC in Japan [29]. The energy resolution at the elastic channel is about 0.06 meV. A helium-3 cryostat was used to access low-temperature regions down to 0.3 K. The $S(Q, E)$ data were reduced using the UTSUSEMI package [30] and visualized in the Mslice module of DAVE [31].

## III. RESULTS AND DISCUSSION

$NaYbO_2$ crystallizes in the rhombohedral delafossite structure with space group $R\bar{3}m$, where $Yb^{3+}$ and $Na^+$ octahedrally coordinated to $O^{2-}$ ions organize a layered structure in the *ab* plane and alternately repeat along the *c* axis. The magnetic layers are well separated to ensure crystallographically their quasi-two-dimensional nature. In the magnetic layer, $Yb^{3+}$ ions form a perfect triangular lattice with a Yb-Yb distance of 3.348 Å. The crystal structural features are drawn in Figs. 1(a)–1(c). The refinement of a neutron powder diffraction pattern confirmed such a structure, and there was no impurity phase observed, as shown in Fig. 1(d). The lattice constants obtained are $a = 3.348$ Å and $c = 16.527$ Å.

The magnetic susceptibility measurements were performed in a temperature range from 0.5 to 380 K, as shown in Fig. 1(e). There is no signature of a magnetic order observed down to 0.5 K. The zero-field-cooled (ZFC) and field-cooled (FC) curves are fully overlapped, which may exclude the possibility of spin freezing [32]. The temperature dependence of the inverse magnetic susceptibility $1/\chi(T)$ in the range from 200 to 380 K is well described by the Curie-Weiss (CW) law, $\chi(T) = \chi_0 + C/(T - \theta_{CW})$, where $\chi_0$ is a temperature-independent residual term, $C$ stands for the Curie constant, and $\theta_{CW}$ is the Curie-Weiss temperature. The fit to the CW law gives $\chi_0 \approx 0.046\,\mathrm{cm}^3/\mathrm{mol}$, $\theta_{CW} = -120$ K, and an effective moment $\mu_{eff} = 4.5\,\mu_B$ derived from $C$. The negative value of $\theta_{CW}$ indicates a strong AFM interaction, which is comparable to the previous results (−100 K), however the residual term $\chi_0$ is much larger [22]. The obtained $\mu_{eff}$ is consistent with the theoretically predicted $4.54\,\mu_B$ for $Yb^{3+}$ ions with the $^2F_{7/2}$ multiplet with $g = 8/7$ [33], as well as with the previous experimental value [22].

The ground-state Kramers doublets of $Yb^{3+}$, resulting from spin-orbit coupling and crystal-electric-field effects, are responsible for the low-temperature magnetic behaviors of $NaYbO_2$ [34]. In addition, quantum fluctuation also has a great impact on the low-temperature magnetic properties of a frustrated spin system [35]. The fit of $1/\chi$ ($T$) in the range from 10 to 20 K to the CW law yields $\chi_0 \approx 0.056\,\mathrm{cm}^3/\mathrm{mol}$, $\theta_{CW} \approx -10$ K, and $\mu_{eff} = 2.4\,\mu_B$. Considering an effective spin-1/2 model, the estimated $g$ factor is 2.77 in terms of $\mu_{eff} = g\sqrt{J(J+1)}\mu_B$, which is close to the average $g$ value (2.86) obtained in the ESR measurements [22]. Its $\theta_{CW}$ of −10 K is very close to the value of −9 K extracted from the ESR analysis [22], whose absolute value is approximately three times bigger than that of $YbMgGaO_4$ [36] ($\theta_{\parallel} = -1.5$ K, $\theta_{\perp} = -2.7$ K), implying much stronger AFM exchange interactions in $NaYbO_2$.

The low-energy spin excitations were examined using the INS technique. $E_i$ of 3.135 meV was selected to map the dynamic structure function $S(Q, E)$ in a desirable reciprocal space with an energy resolution of about 0.06 meV at the elastic channel. The contour plots of $S(Q, E)$ of $NaYbO_2$ are shown in Figs. 2(a)–2(d) at 0.3, 0.6, 1.0, and 2.5 K, respectively. These powder-averaged $S(Q, E)$ spectra are considerably featureless other than a diffuse excitation centered at $Q \sim 1.25\,\text{Å}^{-1}$. The intensity spreads from the elastic line to the high-energy region up to 1.0 meV. As temperature rises,

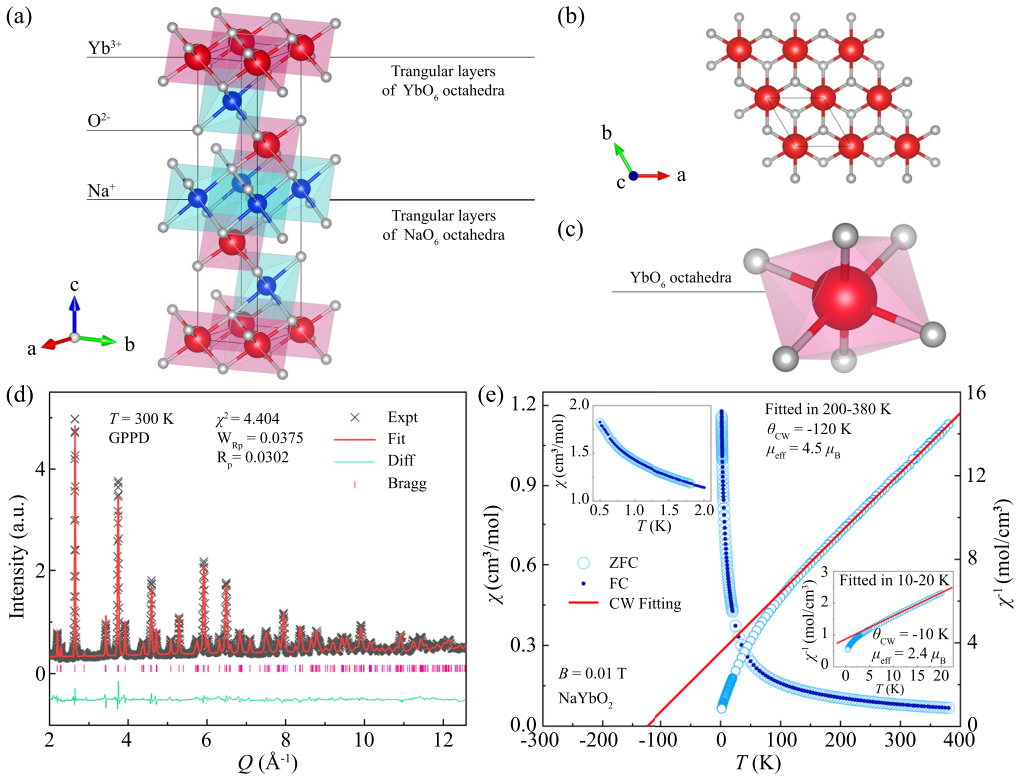


FIG. 1. (a)–(c) Crystal structure of $NaYbO_2$ with the triangular-lattice magnetic layer and $YbO_6$ octahedron highlighted. (d) Neutron powder diffraction pattern of $NaYbO_2$ obtained at GPPD at room temperature and the Rietveld refinement analysis with the $R\bar{3}m$ structure. (e) Magnetic susceptibility of $NaYbO_2$ and the fitting to the CW law. The insets show the magnetic susceptibility and the fitting at the low-temperature region, respectively.

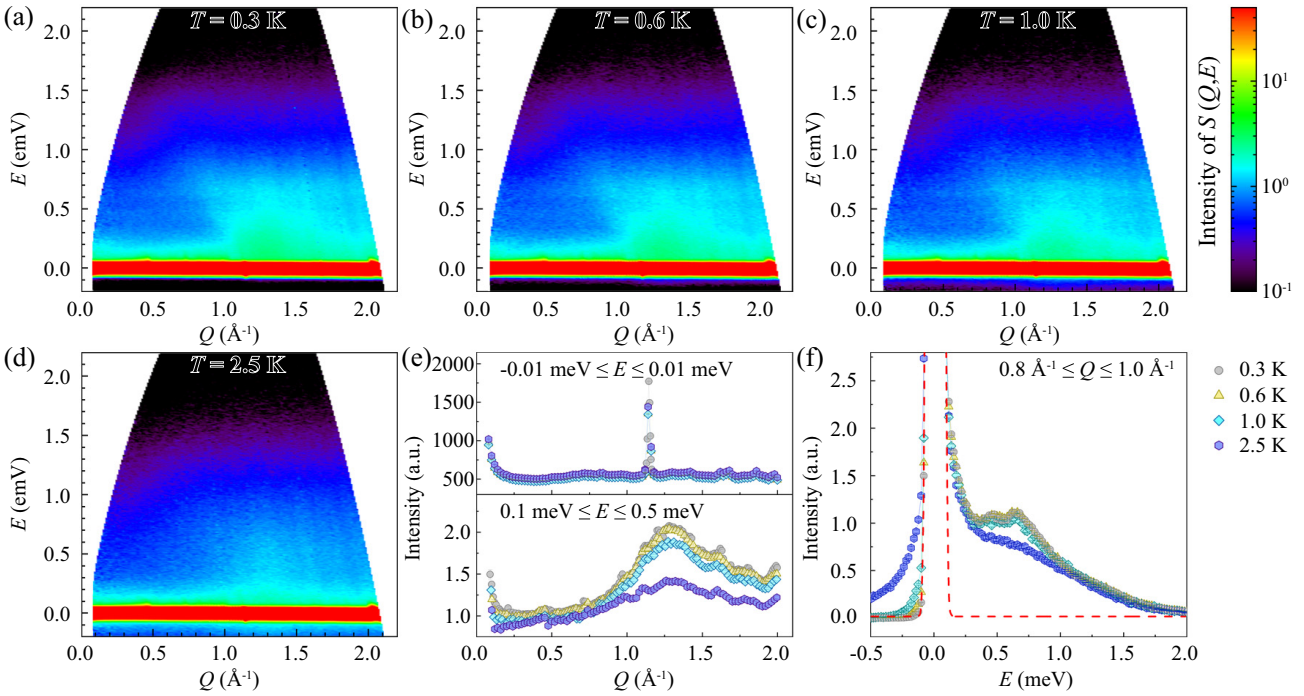


FIG. 2. (a)–(d) Contour plots of dynamic structure function $S(Q, E)$ at 0.3, 0.6, 1.0, and 2.5 K with the incident energy $E_i = 3.135$ meV, respectively. (e) Constant-$E$ cut spectra at $-0.01 \leqslant E \leqslant 0.01$ meV for the elastic component (upper panel) and $0.1 \leqslant E \leqslant 0.5$ meV for the inelastic component (lower panel). (f) Constant-$Q$ cut spectra at $0.8 \leqslant Q \leqslant 1.0$ Å$^{-1}$ with the resolution line plotted.

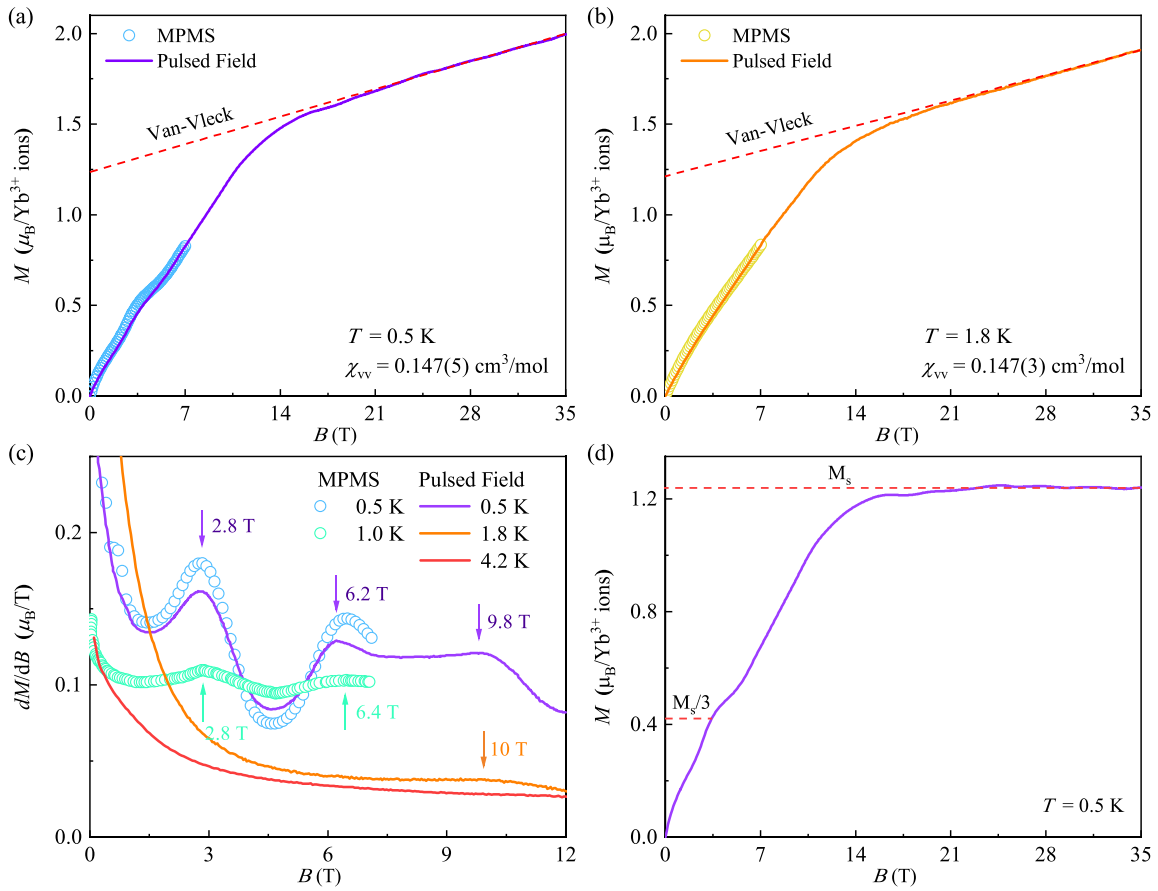


FIG. 3. (a) and (b) Magnetization curves of $NaYbO_2$ at 0.5 and 1.8 K under stationary fields (up to 7 T) and pulse fields (up to 35 T), respectively. The dashed lines represent the Van-Vleck paramagnetic contributions. (c) The differential magnetization ($dM/dB$) curves at 0.5, 1.0, 1.8, and 4.2 K. (d) Magnetization curve at 0.5 K minus the Van-Vleck paramagnetic contribution. The saturated magnetization ($M_s$) and the plateaulike feature at $M_s/3$ are labeled.

the intensity rapidly decays. To examine the spectral details, constant-$E$ and constant-$Q$ cut spectra are plotted in Figs. 2(e) and 2(f), respectively. The elastic peak located at 1.15 $Å^{-1}$ is the (003) nuclear Bragg peak, while the broad inelastic peak observed at 1.25 $Å^{-1}$ is likely attributed to dynamic spin correlations in magnetic layers because this position is related to the magnetic reflection of the propagation vector (1/3,1/3,0). In spectra sliced at $0.8 \leqslant Q \leqslant 1.0\,Å^{-1}$, we observe broad excitations extending up to 2 meV. Within the energy resolution of 0.06 meV, the excitation appears gapless. The shoulder located at about 0.6 meV might be ascribed to complex structures of the spin excitation, which needs to be clarified in a momentum-dependent measurement. It is noted that the excitation bandwidth in $YbMgGaO_4$ is about 1.3 meV [37], which is smaller than 2 meV of $NaYbO_2$ investigated here. This is in agreement with the fact that $NaYbO_2$ has much stronger exchange interactions.

Then, we exploit how such a highly fluctuating state responds to applied magnetic fields and composition tailoring. Shown in Fig. 3(a) is the stationary magnetization curve up to 7 T at 0.5 K. It can be seen that the magnetization is quickly increased, but it is not saturated as the field reaches 7 T. In addition, two anomalies are found at about 3 and 6 T, respectively, which differ from $YbMgGaO_4$ in which a trivial magnetization curve was observed [9]. Such a feature implies that there exist field-induced quantum transitions. Hence, we continue magnetization measurements with pulsed fields up to 35 T. The differential magnetization ($dM/dB$) clearly shows three peaks at 2.8, 6.2, and 9.8 T, and the positions of the first two peaks are consistent with the stationary field magnetization result [Fig. 3(c)]. At 1.8 K, these features become so suppressed that there only exists a very broad bump at about 10 T [see Figs. 3(b) and 3(c)].

The linear behavior of the magnetization curves observed above about 14 T is related to the Van-Vleck paramagnetism. Originating mainly from the excited crystal-electric-field effects, a large Van-Vleck term ($\chi_{vv}$) is usually observed in rare-earth compounds, such as $PrPt_5$ [38] and $Eu_2O_3$ [39]. By extracting the slope of magnetization curve at higher fields, $\chi_{vv}$ are determined to be 0.147(5) and 0.147(3) $cm^3/mol$ for data at 0.5 and 1.8 K, respectively, much larger than previously reported [22]. After subtracting the Van-Vleck term, it can be seen that the system is saturated at about 20 T with the saturation magnetization ($M_s$) of about 1.24 $\mu_B$. This value of $M_s$ is a little smaller than 1.36 $\mu_B$ previously reported in Ref. [22].

It is possible to understand the magnetization process after subtracting the Van-Vleck paramagnetic contribution. As shown in Fig. 3(d), there is a plateaulike feature close to $M_s/3$. $M_s/3$ plateaus have been widely observed in triangular-lattice

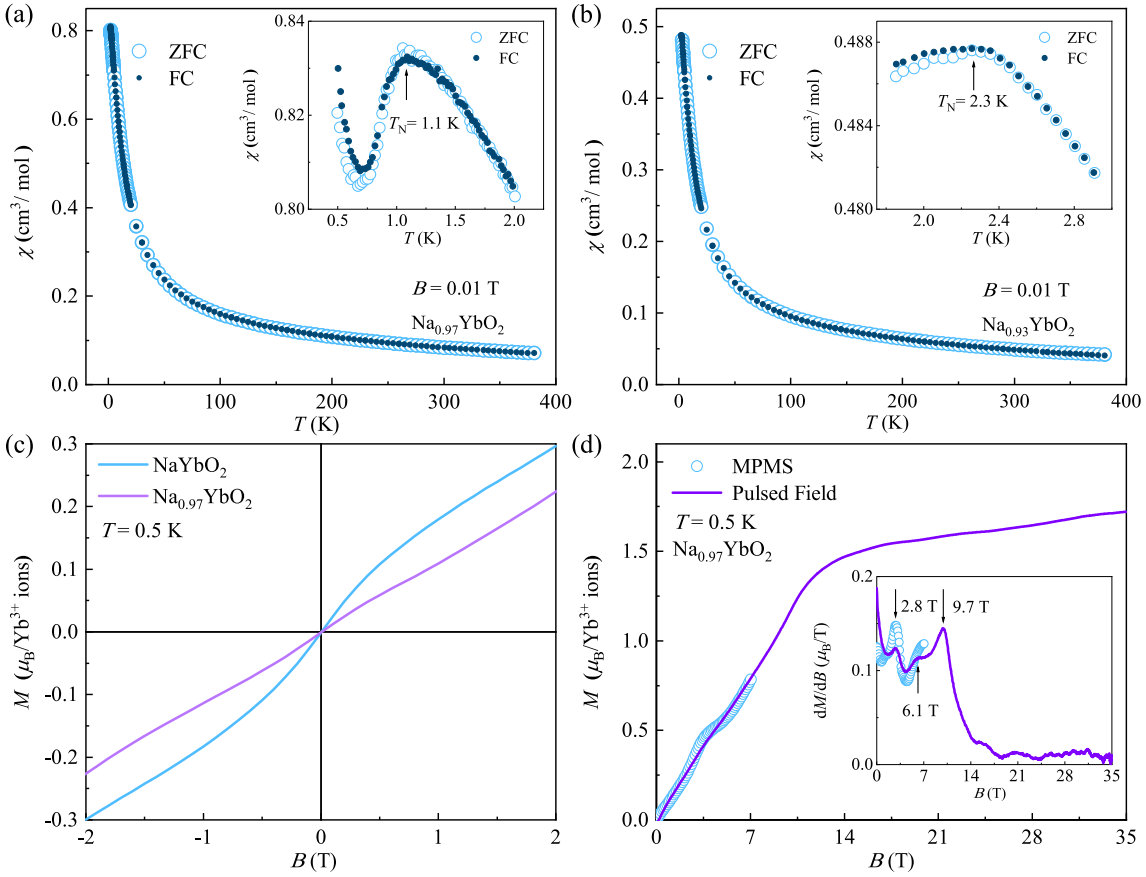


FIG. 4. (a) and (b) Temperature dependencies of magnetic susceptibility of $Na_{0.97}YbO_2$ and $Na_{0.93}YbO_2$, respectively. The insets show the details in the vicinity of the phase transitions with Néel temperatures ($T_N$) labeled. (c) Low-field magnetization curves of $NaYbO_2$ and $Na_{0.97}YbO_2$. (d) Magnetization curves of $Na_{0.97}YbO_2$ at 0.5 K under stationary fields (up to 7 T) and pulsed fields (up to 35 T). The inset shows the differential magnetization ($dM/dB$).

AFM compounds, such as in $RbFe(MoO_4)_2$ [40], $Cs_2CuBr_4$ [41], and $Ba_3CoSb_2O_9$ [42,43]. In a triangular-lattice AFM material with Heisenberg spins, the spins form a 120° AFM spin structure at zero magnetic field [44]. Under an applied magnetic field, such a 120° ordered state is transformed to a collinear up-up-down (*uud*) state with total magnetization equal to $M_s/3$ [45,46]. In addition, quantum spin fluctuations can stabilize the *uud* state over a certain range of field [44]. $NaYbO_2$ differs from these antiferromagnets because its ground state is disordered. The presence of an $M_s/3$ plateaulike feature in $NaYbO_2$ suggests that the disordered state might be suppressed to a 120° AFM structure upon applying magnetic fields. When the magnetic field continues to increase, the *uud* state becomes energetically unstable and then some complex magnetic states appear before spins are fully polarized. Neutron diffraction measurements on $NaYbO_2$ under magnetic fields confirm the existence of the *uud* phase [25,26].

In addition to the influence of magnetic fields, we have also found that the disordered state of $NbYbO_2$ is extremely sensitive to the concentration of $Na^+$ ion vacancies in the compound. Shown in Figs. 4(a) and 4(b) are the temperature dependencies of magnetic susceptibility of $Na_{0.97}YbO_2$ and $Na_{0.93}YbO_2$, respectively. In contrast to the stoichiometric $NaYbO_2$, $Na_{0.97}YbO_2$, and $Na_{0.93}YbO_2$ exhibit magnetic transitions at 1.1 and 2.3 K, respectively. The ZFC and FC curves are not bifurcated at the transition temperatures, which excludes the existence of glassy behavior [32]. We compare the low-field magnetization curves of $NaYbO_2$ and $Na_{0.97}YbO_2$ in Fig. 4(c). $NaYbO_2$ shows a clear nonlinear process, attributed to the suppression of quantum spin fluctuation by magnetic fields. Unlike $NaYbO_2$, $Na_{0.97}YbO_2$ has a smoothing linear magnetization process characteristic of an AFM system. We also examine the high-field magnetization behavior as shown in Fig. 4(d), where $dM/dB$ shows three maxima at 2.8, 6.1, and 9.7 T, respectively, almost identical to the stoichiometric sample. This result also suggests that the disordered state of $NaYbO_2$ is indeed suppressed under very low fields.

Based on the results presented above for field and composition dependencies, we propose putative phase diagrams of the $NaYbO_2$ system. The magnetic quantum disordered state is localized at low temperatures and low fields. With the applied magnetic field increasing, such a state is so fragile that a small magnetic field can transform the system into the 120° AFM state. At about 2.8 T, the 120° spin structure is converted into the collinear *uud* magnetic state, which can be maintained over a certain range of magnetic fields due to the quantum fluctuations. When the magnetic field is higher than 6.2 T, the *uud* state becomes energetically unstable and a canting spin structure is developed. When the applied magnetic field ramps

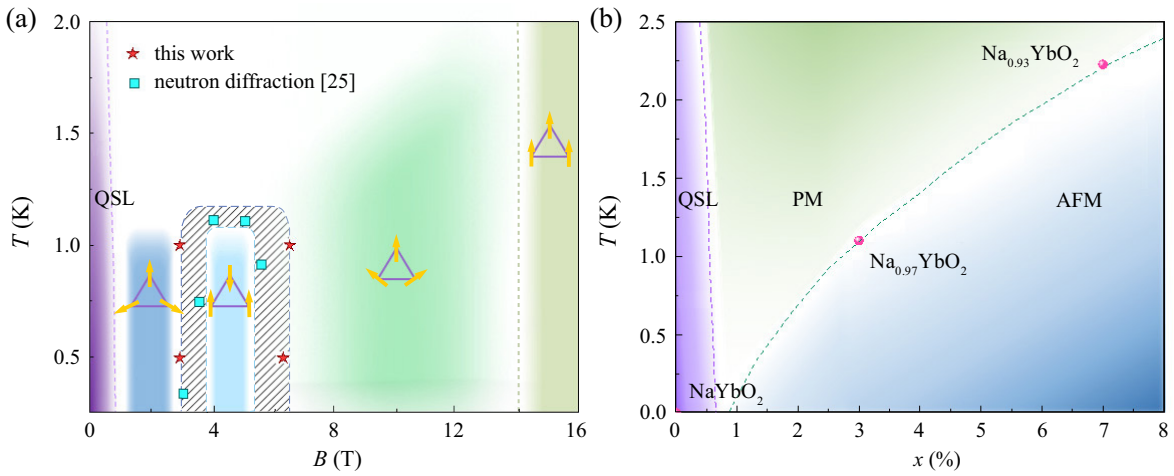


FIG. 5. (a) Field-temperature phase diagram of $NaYbO_2$. The magnetic structures of each state are schematically drawn. Stars denote pulsed-field magnetization measurements. (b) Composition-temperature phase diagram of $Na_{1-x}YbO_2$ system. $T_N$ was determined as shown in Figs. 4(a) and 4(b).

to about 14 T, spins start the gradual crossover to saturation. Finally, spins are fully polarized to form the forced ferromagnetic state at about 20 T. Accordingly, the temperature-field phase diagram is summarized in Fig. 5(a). Similarly, we plot the temperature-composition phase diagram, as shown in Fig. 5(b). The AFM transition temperature decreases with the concentration of $Na^+$ ion vacancies reduced. At a critical point, the concentration of $Na^+$ ion vacancies is not large enough to release the frustration, and then the spin system becomes disordered. These two phase diagrams can serve as a guideline to study this system, but the precise phase boundaries separating the disordered state and this AFM state have not been established yet.

## IV. SUMMARY

To summarize, we have synthesized triangular-lattice AFM $NaYbO_2$, $Na_{0.97}YbO_2$, and $Na_{0.93}YbO_2$. The magnetic properties at low temperatures can be described based on the Kramers doublets. The magnetic susceptibility results indicate strong AFM interactions, and no magnetic order is detected down to 0.5 K. This disordered state is perhaps suppressed to the 120° spin structure, and the $M_s/3$ plateaulike feature is subsequently observed at about 2.8 T. The INS measurements suggest a broad gapless spin excitation persisting up to 2 meV. The vacancies of $Na^+$ ions induce AFM orders in $Na_{0.97}YbO_2$ and $Na_{0.93}YbO_2$ with $T_N$ of 1.1 and 2.3 K, respectively. It is mostly likely that they have a similar 120° spin structure to $NaYbO_2$ in magnetic fields. Our study indicates that $NaYbO_2$ is in very close proximity to the AFM quantum critical point. The magnetic field and composition tunabilities make it a great playground for QSL physics in the future.

## ACKNOWLEDGMENTS

We acknowledge access to the facilities granted by J-PARC (Proposal No. 2018AU1403), CSNS, High Magnetic Field Laboratory of Chinese Academy of Science (Proposal No. 2018-SHMFF-PT-000906), and Wuhan National High Magnetic Field Center (Proposal No. 2018020012). This work has been financially supported by the National Natural Science Foundation of China (Grants No. 11804346 and No. 51771197), the Key Research Program of Frontier Sciences Chinese Academy of Sciences (Grant No. ZDBS-LY-SC002), and the Liaoning Revitalization Talents Program (Grant No. XLYC1807122).

[1] R. Moessner and A. P. Ramirez, Phys. Today **59**(2), 24 (2006).
[2] L. Balents, Nature (London) **464**, 199 (2010).
[3] A. Kitaev, Ann. Phys. **321**, 2 (2006).
[4] O. I. Motrunich and T. Senthil, Phys. Rev. Lett. **89**, 277004 (2002).
[5] L. Balents, M. P. A. Fisher, and S. M. Girvin, Phys. Rev. B **65**, 224412 (2002).
[6] M. Hermele, M. P. A. Fisher, and L. Balents, Phys. Rev. B **69**, 064404 (2004).
[7] Y. Shimizu, K. Miyagawa, K. Kanoda, M. Maesato, and G. Saito, Phys. Rev. Lett. **91**, 107001 (2003).
[8] T. Itou, A. Oyamada, S. Maegawa, M. Tamura, and R. Kato, J. Phys. Condens. Matter **19**, 145247 (2007).
[9] Y. Li, H. Liao, Z. Zhang, S. Li, F. Jin, L. Ling, L. Zhang, Y. Zou, L. Pi, Z. Yang, J. Wang, Z. Wu, and Q. Zhang, Sci. Rep. **5**, 16419 (2015).
[10] Y. Shen, Y. D. Li, H. Wo, Y. Li, S. Shen, B. Pan, Q. Wang, H. C. Walker, P. Steffens, M. Boehm, Y. Hao, D. L. Quintero-Castro, L. W. Harriger, M. D. Frontzek, L. Hao, S. Meng, Q. Zhang, G. Chen, and J. Zhao, Nature (London) **540**, 559 (2016).
[11] Z. Ma, J. Wang, Z.-Y. Dong, J. Zhang, S. Li, S.-H. Zheng, Y. Yu, W. Wang, L. Che, K. Ran, S. Bao, Z. Cai, P. Čermák, A. Schneidewind, S. Yano, J. S. Gardner, X. Lu, S.-L. Yu, J.-M.

Liu, S. Li, J.-X. Li, and J. Wen, Phys. Rev. Lett. **120**, 087201 (2018).
[12] M. R. Norman, Rev. Mod. Phys. **88**, 041002 (2016).
[13] T. Asaba, T. H. Han, B. J. Lawson, F. Yu, C. Tinsman, Z. Xiang, G. Li, Y. S. Lee, and L. Li, Phys. Rev. B **90**, 064417 (2014).
[14] T. H. Han, J. S. Helton, S. Chu, D. G. Nocera, J. A. Rodriguez-Rivera, C. Broholm, and Y. S. Lee, Nature (London) **492**, 406 (2012).
[15] B. Gao, T. Chen, D. W. Tam, C.-L. Huang, K. Sasmal, D. T. Adroja, F. Ye, H. Cao, G. Sala, M. B. Stone, C. Baines, J. A. T. Verezhak, H. Hu, J.-H. Chung, X. Xu, S.-W. Cheong, M. Nallaiyan, S. Spagna, M. B. Maple, A. H. Nevidomskyy, E. Morosan, G. Chen, and P. Dai, Nat. Phys. **15**, 1052 (2019).
[16] I. A. Murav'eva, L. M. Kovba, L. I. Martynenko, and V. I. Spitsyn, Russ. J. Inorg. Chem. **10**, 959 (1965).
[17] Y. Hashimoto, M. Wakeshima, and Y. Hinatsu, J. Solid State Chem. **176**, 266 (2003).
[18] W. Liu, Z. Zhang, J. Ji, Y. Liu, J. Li, X. Wang, H. Lei, G. Chen, and Q. Zhang, Chin. Phys. Lett. **35**, 117501 (2018).
[19] Y. Li, D. Adroja, R. I. Bewley, D. Voneshen, A. A. Tsirlin, P. Gegenwart, and Q. Zhang, Phys. Rev. Lett. **118**, 107202 (2017).
[20] M. Baenitz, Ph. Schlender, J. Sichelschmidt, Y. A. Onykiienko, Z. Zangeneh, K. M. Ranjith, R. Sarkar, L. Hozoi, H. C. Walker, J.-C. Orain, H. Yasuoka, J. van den Brink, H. H. Klauss, D. S. Inosov, and Th. Doert, Phys. Rev. B **98**, 220409(R) (2018).
[21] L. Ding, P. Manuel, S. Bachus, F. Grußler, P. Gegenwart, J. Singleton, R. D. Johnson, H. C. Walker, D. T. Adroja, A. D. Hillier, and A. A. Tsirlin, Phys. Rev. B **100**, 144432 (2019).
[22] K. M. Ranjith, D. Dmytriieva, S. Khim, J. Sichelschmidt, S. Luther, D. Ehlers, H. Yasuoka, J. Wosnitza, A. A. Tsirlin, H. Kühne, and M. Baenitz, Phys. Rev. B **99**, 180401(R) (2019).
[23] K. M. Ranjith, S. Luther, T. Reimann, B. Schmidt, Ph. Schlender, J. Sichelschmidt, H. Yasuoka, A. M. Strydom, Y. Skourski, J. Wosnitza, H. Kühne, Th. Doert, and M. Baenitz, Phys. Rev. B **100**, 224417 (2019).
[24] R. Sarkar, Ph. Schlender, V. Grinenko, E. Haeussler, P. J. Baker, Th. Doert, and H.-H. Klauss, Phys. Rev. B **100**, 241116(R) (2019).
[25] J. Ma, J. Li, Y. Hao Gao, C. Liu, Q. Ren, Z. Zhang, Z. Wang, R. Chen, J. Embs, E. Feng, F. Zhu, Q. Huang, Z. Xiang, L. Chen, E. S. Choi, Z. Qu, L. Li, J. Wang, H. Zhou, Y. Su, X. Wang, Q. Zhang, and G. Chen, arXiv:2002.09224.
[26] M. Bordelon, E. Kenney, T. Hogan, L. Posthuma, M. Kavand, Y. Lyu, M. Sherwin, C. Brown, M. J. Graf, L. Balents, and S. D. Wilson, Nat. Phys. **15**, 1058 (2019).
[27] J. Chen, L. Kang, H. Lu, P. Luo, F. Wang, and L. He, Physica B **551**, 370 (2018).
[28] B. H. Toby, J. Appl. Crystallogr. **34**, 210 (2001).
[29] K. Nakajima, S. Ohira-Kawamura, T. Kikuchi, M. Nakamura, R. Kajimoto, Y. Inamura, N. Takahashi, K. Aizawa, K. Suzuya, K. Shibata, T. Nakatani, K. Soyama, R. Maruyama, H. Tanaka, W. Kambara, T. Iwahashi, Y. Itoh, T. Osakabe, S. Wakimoto, K. Kakurai, F. Maekawa, M. Harada, K. Oikawa, R. E. Lechner, F. Mezei, and M. Arai, J. Phys. Soc. Jpn. **80**, SB028 (2011).
[30] Y. Inamura, T. Nakatani, J. Suzuki, and T. Otomo, J. Phys. Soc. Jpn. **82**, SA031 (2013).
[31] R. T. Azuah, L. R. Kneller, Y. Qiu, P. L.W. Tregenna-Piggott, C. M. Brown, J. R. D. Copley, and R. M. Dimeo, J. Res. Natl. Inst. Stand. Technol. **114**, 341 (2009).
[32] M. J. P. Gingras, C. V. Stager, N. P. Raju, B. D. Gaulin, and J. E. Greedan, Phys. Rev. Lett. **78**, 947 (1997).
[33] I. Sokólska, W. Ryba-Romanowski, S. Gołab, and T. Łukasiewicz, Appl. Phys. B **65**, 495 (1997).
[34] Y.-D. Li, X. Wang, and G. Chen, Phys. Rev. B **94**, 035107 (2016).
[35] S. E. Krüger and J. Richter, Phys. Rev. B **64**, 024433 (2001).
[36] Y. Li, G. Chen, W. Tong, L. Pi, J. Liu, Z. Yang, X. Wang, and Q. Zhang, Phys. Rev. Lett. **115**, 167203 (2015).
[37] J. A. M. Paddison, M. Daum, Z. Dun, G. Ehlers, Y. Liu, Ma. B. Stone, H. Zhou, and M. Mourigal, Nat. Phys. **13**, 117 (2017).
[38] K. Andres and E. Bucher, J. Appl. Phys. **42**, 1522 (1971).
[39] H. Samata, N. Wada, and T. C. Ozawa, J. Rare Earth. **33**, 177 (2015).
[40] L. E. Svistov, A. I. Smirnov, L. A. Prozorova, O. A. Petrenko, L. N. Demianets, and A. Ya. Shapiro, Phys. Rev. B **67**, 094434 (2003).
[41] T. Ono, H. Tanaka, H. Aruga Katori, F. Ishikawa, H. Mitamura, and T. Goto, Phys. Rev. B **67**, 104431 (2003).
[42] Y. Shirata, H. Tanaka, A. Matsuo, and K. Kindo, Phys. Rev. Lett. **108**, 057205 (2012).
[43] Y. Kamiya, L. Ge, T. Hong, Y. Qiu, D. L. Quintero-Castro, Z. Lu, H. B. Cao, M. Matsuda, E. S. Choi, C. D. Batista, M. Mourigal, H. D. Zhou, and J. Ma, Nat. Commun. **9**, 2666 (2018).
[44] M. Lee, J. Hwang, E. S. Choi, J. Ma, C. R. De la Cruz, M. Zhu, X. Ke, Z. L. Dun, and H. D. Zhou, Phys. Rev. B **89**, 104420 (2014).
[45] J. Alicea, A. V. Chubukov, and O. A. Starykh, Phys. Rev. Lett. **102**, 137201 (2009).
[46] A. V. Chubukov and D. I. Golosov, J. Phys.: Condens. Matter. **3**, 69 (1991).